Vol. 88 No. 6 pp. 1653–1664 ACTA GEOLOGICA SINICA (English Edition) Dec. 2014

Braincase Anatomy of the Basal Theropod *Sinosaurus* from the Early Jurassic of China

XING Lida[1,*], Ariana PAULINA-CARABAJAL[2,*], Philip J. CURRIE[3], XU Xing[4], ZHANG Jianping[1], WANG Tao[5], Michael E. BURNS[3] and DONG Zhiming[4]

1 *School of the Earth Sciences and Resources, China University of Geosciences, Beijing 100083, China*
2 *Museo Carmen Funes, Consejo Nacional de Investigaciones Científicas y Tecnológicas, Av. Córdoba 55 (8318), Plaza Huincul, Neuquén, Argentina*
3 *University of Alberta, CW405 Biological Sciences Building, Edmonton, Alberta T6G 2E9, Canada*
4 *Institute of Vertebrate Paleontology and Paleoanthropology, Chinese Academy of Sciences, Beijing 100044, China*
5 *Lufeng Land and Resources Bureau, Lufeng 651200, China*

Abstract: The neuroanatomy of the mid-sized theropod *Sinosaurus triassicus* from the Lower Jurassic Lufeng Formation, Lufeng Basin in Yunnan Province, China was studied using X-ray computed tomography. The braincase is characterized by a large supraoccipital knob that is capped by a posterior projection of the parietal and two external foramina for the caudal middle cerebral vein, which is completely enclosed by the supraoccipital. The basicranium has well defined, short basipterygoid processes that project ventral to the basal tubera. The basisphenoid is expanded, projects posteroventrally, and is pierced by four pneumatic recesses. The endocranial morphology resembles that observed in other basal theropods—in particular some allosauroids—and has a strongly marked pontine flexure and a large dorsal expansion. The inner ear morphology is also similar to that observed in other basal theropods, with slender semicircular canals. The anterior semicircular canal is 20% larger than the posterior semicircular canal, and the angle formed between them is less than 90° when seen in dorsal view.

Key words: Neuroanatomy, paleoneurology, Dinosaur, inner ear, pneumaticity, Early Jurassic, Yunnan

1 Introduction

Sinosaurus triassicus (="*Dilophosaurus sinensis*") (Hu, 1993) is an Early Jurassic theropod from China, which is characterized by twin hatchet-shaped crests similar to those of its North American relative *Dilophosaurus* (Hu, 1993; Dong, 2003; Xing et al., 2013). *Sinosaurus* already havs be reported from four bone site (Xing, 2012) and one probably tracksite (Xing et al., 2009; Lockley et al., 2013) from the Lower Jurassic Lufeng Formation in the Lufeng Basin in Yunnan Province, southeastern China. Recent phylogenetic analyses, based on new specimens show that *Sinosaurus triassicus* is not the most basal dilophosaurid (Smith et al., 2007), but is more closely related to *Averostra* than to *Coelophysis bauri* and *Dilophosaurus wetherilli* (Rauhut, 2003; Xing, 2012; Xing et al., 2013; Xing et al., in press). In this study, we present for the first time, a detailed description of the neuroanatomy of *Sinosaurus triassicus*.

Studies on the paleoneurology of dinosaurs are possible using natural or artificial endocasts. However, well-preserved braincase specimens, especially in basal theropods are rare and the brain and inner ear morphology of basal theropods is as yet poorly known. The paleoneurology of a few taxa has been studied, including the coelophysoid *Coelophysis rhodesiensis* (Raath, 1977, fig. 23), allosauroids *Allosaurus fragilis* (Rogers, 1999), *Carcharodontosaurus saharicus* (Larsson, 2001), *Acrocanthosaurus atokensis* (Franzosa and Rowe, 2005), *Giganotosaurus carolinii* (Paulina Carabajal and Canale, 2010) and *Sinraptor dongi* (Paulina Carabajal and Currie, 2012), and ceratosaurs *Ceratosaurus nasicornis* (Sanders and Smith, 2005), *Majungasaurus crenatissimus* (Sampson and Witmer, 2007) and *Aucasaurus garridoi* (Paulina Carabajal and Succar, in press). Of this sample,

* Corresponding author. E-mail: xinglida@gmail.com
premjisaurus@yahoo.com.ar

only four of the taxa are Jurassic in age and, therefore, the new information on the neuroanatomy of *Sinosaurus triassicus* will facilitate comparison with the other basal theropods with known braincases, and aid further understanding of neuroanatomy within basal theropods.

Institutional abbreviations: KMV, Kunming City Museum, Kunming, Yunnan, China; **LDM**, Lufeng Dinosaurian Museum, Lufeng, Yunnan, China; **MCF-PVPH**; Museo "Carmen Funes", Plaza Huincul, Neuquén, Argentina; **PVL**, Instituto Miguel Lillo, Tucumán, Argentina; **UCMP**, University of California, Museum of Paleontology, Berkeley, USA; **ZLJ**, Lufeng World Dinosaur Valley Park, Yunnan, China.

2 Material and Methods

In the case of *Sinosaurus triassicus* the braincase has been preserved in several specimens (e.g. KMV 8701 and LDM L10) but many areas are obscured by sediment (due to the poorly preparation, Xing, 2012), which is the reason why this part of the skull has remained undescribed in this taxon (Hu, 1993). Recently, an almost complete braincase (ZLJT01) has been prepared and studied by one of the authors (Xing, 2012). This braincase has allowed the description of most of the vascular and cranial nerve foramina and delicate structures, such as basipterygoid and cultriform processes, which are often missing in other theropod braincases.

More recently the braincase has been CT scanned facilitating the description of the endocranial morphology (brain, inner ear, and pneumaticity) of this taxon. The braincase (ZLJT 01) was CT scanned using a SOMATOM Definition AS/AS+ with FAST CARE (64-slice and 128-slice config.) at Central Hospital, Chaozhou City, Guangdong Province, China. The slice thickness was 600 μm at 120 kV and 350 mA. Virtual three-dimensional inner ear and cranial endocasts were made by one of the authors (APC) using the software Materialise Mimics (version 14.0).

Comparisons with other basal theropod endocasts were based on the first-hand observation of *Aucasaurus garridoi* (Paulina Carabajal, 2011a, Paulina Carabajal and Succar, in press), *Giganotosaurus carolinii* (Paulina Carabajal and Canale, 2010) and *Sinraptor dongi* (Paulina Carabajal and Currie, 2012); and published descriptions of *Acrocanthosaurus* (Franzosa and Rowe, 2005), *Allosaurus* (Franzosa, 2004), *Ceratosaurus* (Sanders and Smith, 2005), *Majungasaurus crenatissimus* (Sampson and Witmer, 2007) and *Syntarsus kayentakatae* (Rowe, 1989). As proposed by Witmer et al. (2008), we will refer to the digital casts of structures as if they were the structures themselves (e.g., ''olfactory bulb'' instead of ''olfactory bulb cavity endocast'').

3 Braincase

The braincase (Fig. 1) is exceptionally well preserved and almost complete, missing only the orbitosphenoids and the ethmoidal elements, which may not have been ossified elements, as in other theropods (e.g. Paulina Carabajal and Currie, 2012). The skull roof has partial parietals fused to the occipital section of the braincase, and an isolated frontal. The empty endocranial cavity is exposed anterodorsally. The occiput is complete, except for the most dorsal part of the supraoccipital knob and the lateral expansions of the exoccipital-opisthotic complex (paroccipital processes), which are crushed. The foramen magnum is dorsoventrally deformed and, as preserved, is approximately 3.2 cm wide and 1.7 cm high (Fig. 1B). The occipital condyle is formed mainly by the basioccipital and laterodorsally by the exoccipitals. It is semicircular in posterior view, being 40 mm wide and 30 mm height. The sutures on the occiput are not completely closed, suggesting that the specimen is a sub-adult individual. Delicate structures such as the preotic pendant, basipterygoid processes and cultriform process are preserved.

3.1 Parietal. Both parietals are fused forming a single midline element in the skull roof. Anteriorly, the interdigitating fronto-parietal suture is mostly transverse to the sagittal axis of the skull. Although the dorsal surface of the parietal is eroded, the morphology of the posterior section of the skull roof suggests that the fused parietals formed a relatively wide (transversely), dorsally flat sagittal bar between the supratemporal fossae (Figs. 1-2). The narrowest distance between the supratemporal fenestrae is 27 mm (Fig. 2). Each supratemporal fossa is deeply excavated on the surface of the parietal.

The nuchal crest is incomplete, although the preserved sections indicate that it was "V" shaped in dorsal view, with slender and low posterolateral wings overlapping dorsally the base of the paroccipital processes (Fig. 1B). Posteriorly, the parietal forms a median tongue-shaped process that posteriorly overlaps the supraoccipital knob (Figs. 1A, 2). This character is also observed in carcharodontosaurids (Coria and Currie, 2002a), neoceratosaurids (Bonaparte, 1991; Paulina Carabajal, 2011a, b; Sampson and Witmer, 2007) and sinraptorids (Currie and Zhao, 1993).

3.2 Frontal. The left frontal is preserved separately from the rest of the braincase. It is almost complete, and missing only the nasal process anteriorly (Fig. 3). The frontal is anteroposteriorly long and triangular in shape, with a maximum width of 72 mm on the frontoparietal

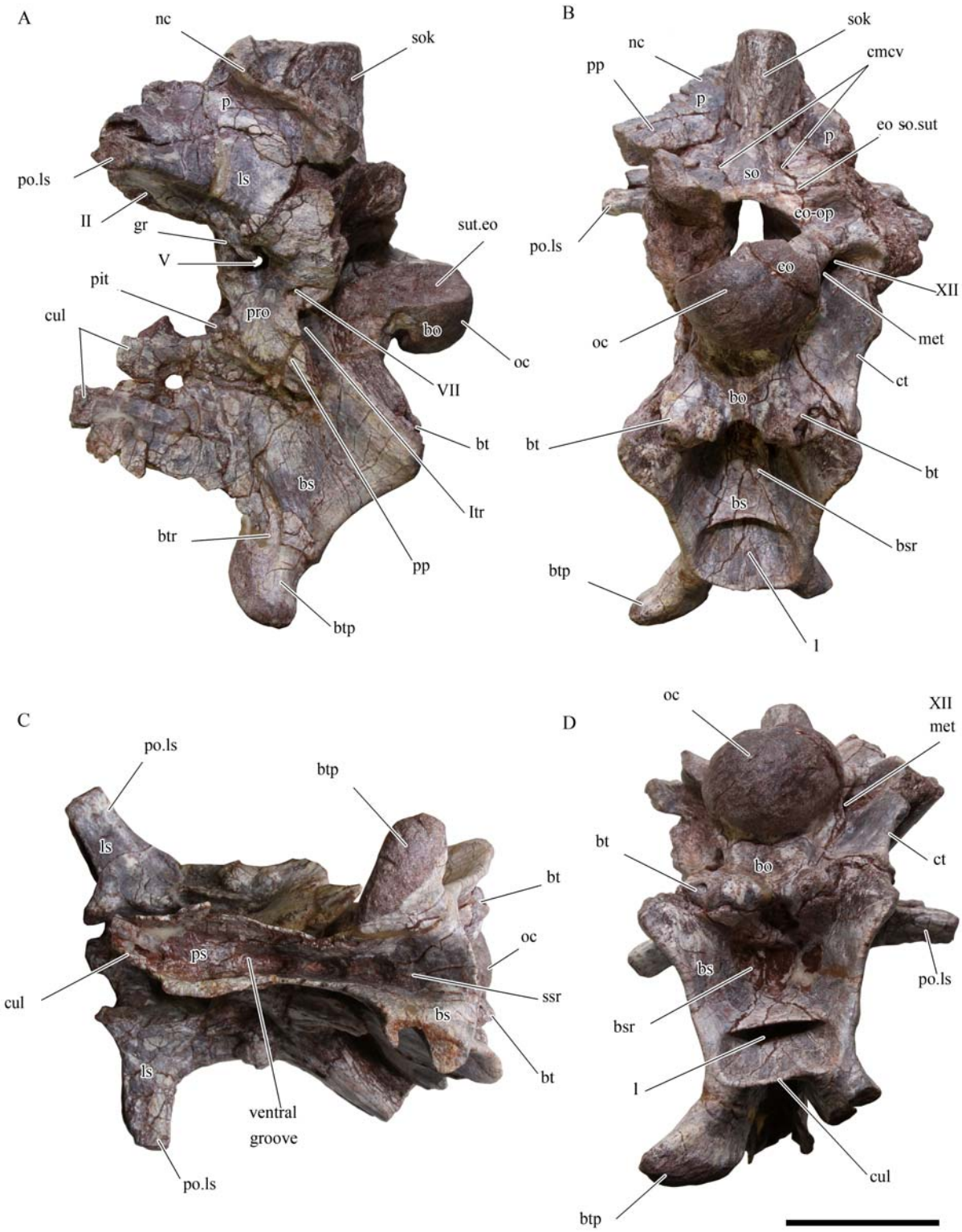

Fig. 1. Braincase of *Sinosaurus triassicus* (ZLJT01) in left lateral (A), posterior (B), ventral (C) and posteroventral (D) views. Abbreviations: bs, basisphenoid; bsr, basisphenoidal recess; bt, basal tuber; btp, basipterygoid process btr, basipterygoid recess; cmcv, caudal middle cerebral vein; ct, crista tuberalis; cul, cultriform process; eo-op. sut, suture surface for the exoccipital-opisthotic complex; f, frontal; gr, groove; ls, laterosphenoid; met, methotic foramen (for cranial nerves IX-XI); nc, nuchal crest; ps, parasphenoid; pit, pituitary fossa; oc, occipital condyle; p, parietal; pp, posterolateral wing of parietal; po.ls, postorbital process of laterosphenoid; pp, preotic pendant; pro, prootic; so, supraoccipital; sok, supraoccipital knob; 1, secondary pneumatic recess within the basisphenoidal recess; II, V, VII, XII, cranial nerve foramina. Scale bar equals 5 cm.

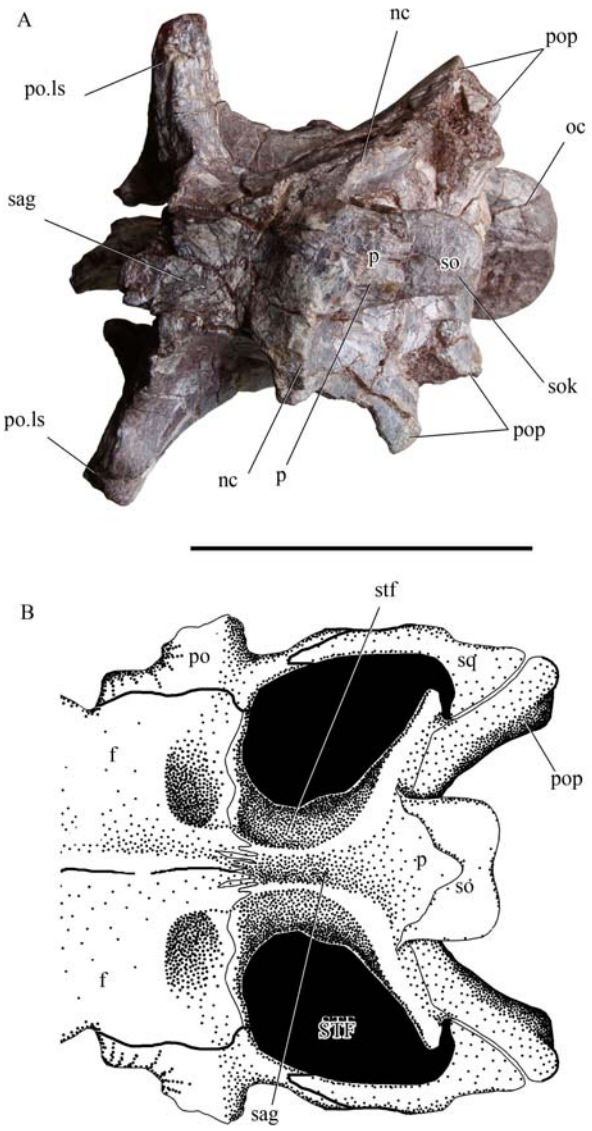

Fig. 2. Braincase of *Sinosaurus triassicus* (ZLJT01) in dorsal view (A), drawing reconstruction of the skull roof (B). Abbrevitions: f, frontal; nc, nuchal crest; oc, occipital condyle; p, parietal; po, postorbital; po.ls, postorbital process of laterosphenoid; pop, paroccipital process; sag, sagittal bar; sok, supraoccipital knob; sq, squamosal; stf, supratemporal fossa; STF, supratemporal fenestra. Scale bar equals 5 cm.

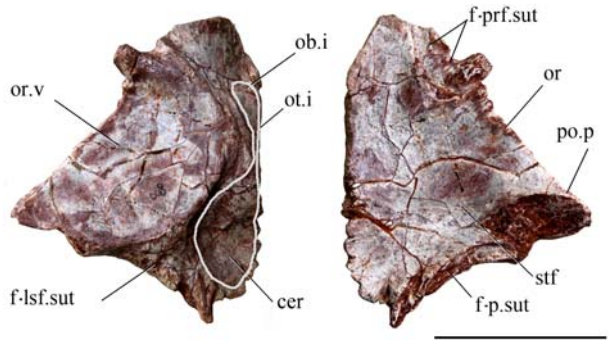

Fig. 3. Right frontal of *Sinosaurus triassicus* (ZLJT01) in ventral (A) and dorsal (B) views. Abbreviations: or.v, orbital vault; ob.i, olfactory bulb impression; ot.i, olfactory tract impression; cer, cerebral hemisphere cavity; f-ls.sut, suture surface for the laterosphenoid; f-prf.sut, suture surface for the prefrontal; or, orbital rim; po.p, postorbital process; stf, supratemporal fossa; f-p.sut, suture surface for the parietal. Scale bar equals 5 cm.

suture and a maximum length of 82 mm measured on the interfrontal suture. The dorsal surface of the bone is smooth and mostly flat. Posteriorly, the anterior margin of the supratemporal fossa has only limited extension onto the dorsal surface of the frontal (Fig. 3A).

The postorbital process of the frontal projects markedly posterolaterally, clearly differentiated from the lateral margin of the frontal in dorsal view (Fig. 3B). The elongated anteroposterior separation of the postorbital process and the prefrontal suture indicate that the frontal participated largely on the dorsal margin of the orbit.

On the ventral aspect of the frontal, the surface of contact with the laterosphenoid is a triangular area (Fig. 3A). There, the cerebral impression is shallow and oval-shaped (Fig. 3A) separated by a constriction from the olfactory tract and the smooth olfactory bulb impression, which is divergent from the midline. The length of the cerebral hemisphere impression is 42 mm, whereas the length of the olfactory bulb cavity is 25 mm.

The morphology of the frontal of specimen ZLJT01 is similar to those in LM-L10 and KMV 8701. The frontals of *Dilophosaurus wetherilli* (UCMP 37302; Welles, 1984) are poorly preserved and too badly distorted for further comparison.

3.3 Supraoccipital. The supraoccipital is three times the height (62 mm) of the foramen magnum (Fig. 1B). The distinct supraoccipital knob has a posterodorsally expanded median ridge, which is less prominent than those in *Allosaurus* (Madsen, 1976), *Sinraptor* and *Yangchuanosaurus* (Currie and Zhao, 1993). In *Sinosaurus* the supraoccipital knob occupies 60% of the height of the supraoccipital bone. The dorsal surface of this knob is flat, smooth and triangular in dorsal view. Lateral to the supraoccipital knob, there is a pair of vascular foramina on each side, completely enclosed by the supraoccipital (Figs. 1B, 4). The most dorsal foramen (for the dorsal head vein) is circular and has a smaller diameter than the ventral foramen (for the caudal middle cerebral vein), which is teardrop shaped. The CT scans show that the passages for both the caudal middle cerebral vein and the dorsal head vein are confluent internally and form a single passage that enters the dural peak. In most theropods, the dorsal head vein exits the braincase

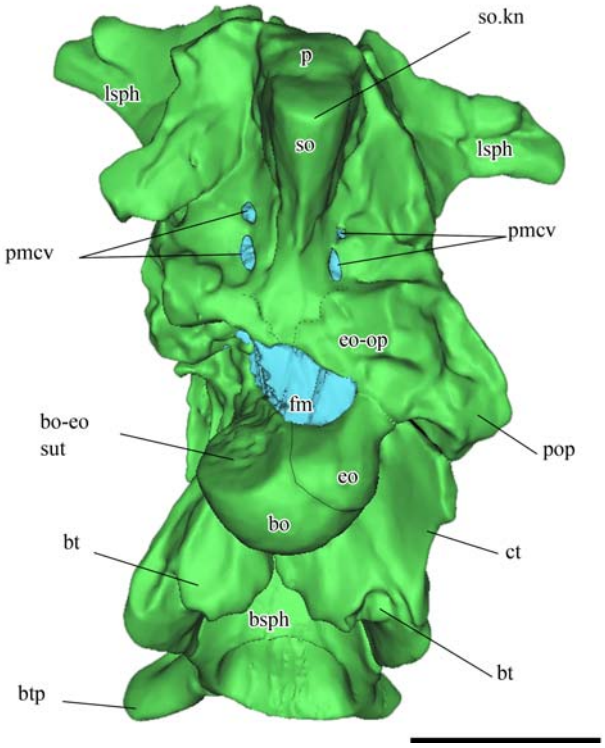

Fig. 4. Volume-rendered CT-based reconstruction of the braincase of *Sinosaurus triassicus* (ZLJT01) in slightly posterodorsal view. Details of the head vasculature and basisphenoidal recess. Abbreviations: bo, basioccipital; bo-eo.sut, suture surface for the exoccipital; bt, basal tuber; btp, basipterygoid process; ct, crista tuberalis; eo, exoccipital; eo-op, exoccipital-opisthotic complex; lsph, laterosphenoid; p, parietal; pmcv, caudal middle cerebral vein; pop, paroccipital process; so, supraoccipital; so.kn, supraoccipital knob. Scale bar equals 5 cm.

laterally in a foramen within the adductor chamber between laterosphenoid, parietal, and prootic (Witmer and Ridgely, 2010). The exit of the dorsal head vein on the occiput could represent an autamomorphy for *Sinosaurus*. An anastomosis of the dorsal head vein and the caudal middle cerebral vein within the skull has been described for *Majungasaurus* (Sampson and Witmer, 2007).

Although the sutures with the exoccipital-opisthotic complex are not clear, the supraoccipital seems to have a limited participation on the dorsal margin of the foramen magnum. The supraoccipital, however, is excluded from the dorsal margin in *Dilophosaurus* (Welles, 1984).

3.4 Exoccipital-opisthotic. The exoccipitals are separated from each other by a small ventral extension of the supraoccipital above the foramen magnum. The left exoccipital-opisthotic complex is missing, leaving the exoccipital-opisthotic suture on the basioccipital exposed (Figs. 1B, 4). As in other known theropods, there is no evident division between the exoccipital and the opisthotic (Currie, 1997), which are firmly fused together.

The right proximal section of the paroccipital process, which is formed mainly by the opisthotic, is 84 mm tall. Fractures (and the CT scans) show that the paroccipital process is a solid structure. In posterior view, the ventral border of the paroccipital process is level with the ventral border of the occipital condyle, as in *Sinosaurus* specimens KMV 8701and LDM–L10, *Cryolophosaurus* (Smith et al., 2007) and the allosauroid *Sinraptor* (Currie and Zhao, 1993). The ventral border is level with the dorsal margin of the occipital condyle in *Carnotaurus* (Paulina Carabajal, 2011b), *Dilophosaurus* (Welles, 1984) and *Syntarsus* (Tykoski, 1998).

The anterior surface of the paroccipital process is smooth, and there is no caudal tympanic recess between the opisthotic and the prootic. The opisthotic contacts the prootic anteriorly, although there are no visible sutures. Both elements form an expanded and rounded surface, which overhangs a triangular recess that houses the columellar recess anteriorly and another two foramina posteriorly; the columellar recess is small and circular. The foramen posterior to this recess probably corresponds to cranial nerve (CN) IX; the second foramen is probably a product of damage, because the CT scans do not show an internal connection between it and the endocranial cavity.

The crista tuberalis, formed by the ventral ramus of the opisthotic, is well developed and distally reaches the tip of the basal tuber. It is a well-developed lamina that separates the posterior and lateral surfaces of the braincase. The sutural contact with the basioccipital posteriorly and the basisphenoid anteriorly are clearly visible (Fig. 1A,D).

Lateral to the occipital condyle, and delimited anteriorly by the crista tuberalis, there is an oval recess that houses two foramina: one foramen for CN XII and the other corresponding to the metotic foramen, which houses at least CN X, XI and the jugular vein, as in other theropods (Currie, 1997). The dorsal margin of this recess is formed by a bar of bone that overhangs the foramina, so that it is not visible in posterior view; this is also the case in *Sinraptor dongi* (Paulina Carabajal and Currie, 2012). Cranial nerve IX, as mentioned above, has a separate foramen anterior to the crista tuberalis, on the lateral side of the braincase. A lateral opening in the braincase for this nerve (separate from the more posterior metotic foramen) is also present in the abelisaurid *Abelisaurus* (Paulina Carabajal, 2011a) and an unnamed theropod (MCF-PVPH 411) from the Cretaceous of Patagonia (Coria and Currie, 2002b; Paulina Carabajal, 2009).

3.5 Basioccipital. The basioccipital forms most of the occipital condyle and the basal tubera. The transverse

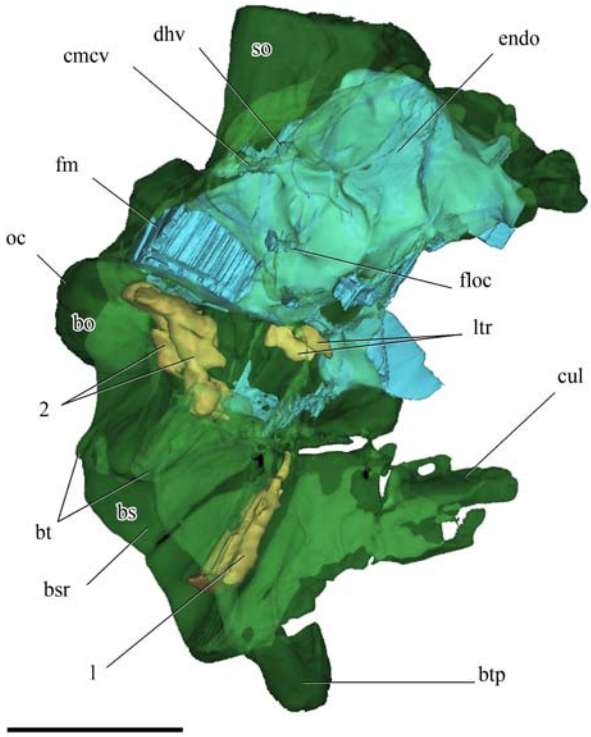

Fig. 5. Volume-rendered CT-based reconstruction of the skull, endocranial cavity and pneumatic recesses of *Sinosaurus triassicus* (ZLJT01). The bone is rendered semitransparent to show the endocranial cavity. Abbreviations: bsr, basisphenoidal recess; bt, basal tuber; cmcv, caudal middle cerebral vein; endo, endocranial cast; cul, cultriform process; floc, floccular process; fm, foramen magnum; ltr, lateral tympanic recess; oc, occipital condyle; ts, transversal sinus; 1, secondary pneumatic recess within the basisphenoidal recess; 2, pneumatic cavity in the neck of the occipital condyle. Scale bar equals 5 cm.

distance across the basal tubera (52 mm) is larger than the transverse diameter of the occipital condyle (42 mm). The basal tubera are separated by a shallow ventral depression and are slightly divergent (Fig. 1B). The surface ventral to the occipital condyle is flat and smooth, and there is no subcondylar recess. Each basal tuber is formed by the basioccipital posteriorly and the basisphenoid anteriorly (Fig. 1B, D).

The neck of the occipital condyle is flat dorsally and has no dorsal longitudinal groove, unlike *Dilophosaurus* (Welles, 1984). A shallow paracondylar recess is lateral to the occipital condyle, whereas *Cryolophosaurus*, *Dilophosaurus* and *Syntarsus kayentakatae* have well-developed paracondylar pockets (Welles, 1984; Tykoski, 1998; Smith et al., 2007). The CT scans show paired pneumatic cavities inside the neck of the occipital condyle, which are principally within the basioccipital (Fig. 5).

3.6 Basisphenoid–Parasphenoid. The basisphenoid is complete and fused anteriorly to the parasphenoid. The only sutures clearly visible in the braincase are those with the basioccipital posteriorly and the opisthotic dorsally (Fig. 1A).

The cultriform process, which is probably formed mainly by the parasphenoid, is incomplete anteriorly. The cultriform is a long process with a tall base, and is projected slightly anterodorsally when complete. The preserved section of the cultriform process is equal in length to the anteroposterior length of the basicranial box. The process is formed by two thin and longitudinal webs of bone that converge and join dorsally, arching over a ventrally oriented longitudinal groove, as observed in *Piveteausaurus* (Taquet and Welles, 1977), *Poekilopleuron*? (Allain, 2002), and *Sinraptor* (Paulina Carabajal and Currie, 2012). In *Sinosaurus*, this groove is connected posteriorly to the subsellar recess, which is excavated on the basisphenoid (Fig. 1C).

The basisphenoid forms the anterior section of the basal tubera and the body of the basipterygoid processes. The latter are short, finger-like, and project laterally (Fig. 1A,B). They are joined transversally by the basipterygoidal web but have free distal ends. The distal end of each process has an oval surface with two distinct facets for the contact with the pterygoid bone. It is a short process but is well differentiated from the body of the basisphenoid in lateral view. There is an oval depression on the lateral surface of each process that corresponds to the basipterygoid recess observed in other theropods (Fig. 1A). However, this depression is not connected internally with pneumatic cavities. Fractures and CT scans show that the basipterygoid processes are solid structures, not affected by pneumaticity. The basipterygoid recess is present in many other theropods, such as *Allosaurus* (Madsen, 1976), *Oviraptor* (Norell et al., 2001), ? *Stokesosaurus* (Chure and Madsen, 1998), and *Velociraptor* (Barsbold and Osmólska, 1999).

The basisphenoid recess is a large and deep cavity on the ventral aspect of the basisphenoid. The recess is subrectangular in ventral view, delimited between the basal tubera and the basipterygoid processes, and opens posteroventrally (Fig. 1D). Strikingly, the basisphenoid recess is subdivided anteriorly by a delicate lamina of bone just behind the basipterygoid processes, forming an elongated pocket with distinct margins. The main opening of the basisphenoidal recess has two irregular foramina in connection with a pair of pneumatic cavities at the level of the neck of the occipital condyle. The smaller subdivision (identified as “1” in Figs. 1B,D) is a transversely developed conical recess, invading the basisphenoid. Internally, it is not in connection with other pneumatic cavities. Although the presence of a single foramen or paired foramina within the basisphenoidal recess is not

uncommon, the presence of an extra transverse web of bone subdividing the recess seems to be an autapomorphy for this taxon. *Sinraptor* exhibits extra pneumatic cavities in the same region within the basisphenoidal recess, although they are paired cavities that do not connect medially (Paulina Carabajal and Currie, 2012).

The lateral tympanic recess is a deep, narrow pneumatic cavity excavated laterally into the basisphenoid, and extending posteroventrally to the preotic pendant (Fig. 1A). The preotic pendant seems to be formed mainly by the basisphenoid, and is a well-developed laminar process overhanging the anterodorsal portion of the lateral tympanic recess. This recess is an irregular chamber, separated from a ventral depression by a low ridge, which more closely resembles the situation observed in *Sinraptor* than in other theropods such as *Abelisaurus* (Paulina Carabajal, 2011b), *Piatnitzkysaurus* (PVL 4073; Rauhut, 2004), and *Troodon* (Currie, 1985); in the latter, the lateral tympanic recess is larger, has well demarcated borders, and is deep and subdivided into many chambers. The CT scans show that the foramen for the internal carotid artery is located within this recess.

The posterior half of the pituitary fossa is preserved in the basisphenoid. The dorsum sella is low and projects slightly anterodorsally. Only the posterior margin of the infundibulum is preserved and it is not possible to determine its diameter. The internal carotid artery enters the pituitary fossa posteroventrally, and is separate from its counterpart. The CN VI foramina open on the posterior wall of the pituitary fossa, dorsal to the internal carotid foramina.

3.7 Prootic. The prootic is complete and there are no visible sutures with the opisthotic, basisphenoid or laterosphenoid. Close to the parietal suture dorsal to CN V, there is a vascular foramen, which transmitted the middle cerebral vein. The prootic seems to form only a small dorsal portion of the large preotic pendant that extends anteroventrally from the main body of the prootic, obscuring the foramen for the internal carotid.

The foramen for CN V is circular and the largest in the braincase. It is enclosed between the prootic and the laterosphenoid. There is a groove on the lateral surface of the laterosphenoid extending anterodorsally from the CN V foramen, indicating the path of the ophthalmic branch (V_1). If there was a lamina that laterally enclosed the groove, then there would have been a separate ophthalmic branch from the maxillary and mandibular branches of the trigeminal nerve.

Cranial Nerve VII is completely enclosed by the prootic. It is oval in outline and posterior to CN V. There are well-marked dorsal and ventral grooves running from the foramen, indicating the paths for the hyomandibular and maxillary branches of the nerve (Fig. 1A), as in *Dilophosaurus* (Welles, 1984), *Irritator* (Sues et al. 2002) and *Piatnitzkysaurus* (PVL 4073).

The posterior branch of the prootic ventrally delimits an oval recess excavated mainly on the opisthotic. Within this recess open two foramina separated by a vertical thin lamina of bone. The anterior smaller foramen corresponds to the columellar recess, which is bounded anteriorly by the prootic and posteriorly by the opisthotic. As previously mentioned, the posterior foramen probably corresponds to a separate CN IX.

3.8 Laterosphenoid. The laterosphenoid is incomplete anteroventrally. There are no visible sutures with the prootic posteriorly and the orbitosphenoid is missing anteriorly.

The postorbital process of laterosphenoid is a dorsolaterally projecting structure, which is dorsoventrally depressed; as suggested by the latersphenoid–frontal suture, it probably extended beyond the postorbital process of the frontal. On the ventral surface of the base of the postorbital process, there is a shallow but large oval impression that indicates the contact with the epipterygoid bone (Fig. 1C).

The margins of a small foramen are preserved at the level of the postorbital process on each side, and might correspond to CN IV. The foramina for CN II (enclosed by the orbitosphenoids) and CN III (enclosed posteriorly by the laterosphenoid) are not preserved in the specimen.

3.9 Braincase pneumaticity. Four pneumatic recesses are present in the basicranium: the basipterygoid recess, the subsellar recess, the basisphenoidal recess and the lateral tympanic recess (Fig. 5).

The lateral tympanic recess is poorly developed on the lateral surface of the basisphenoid, as shown by the CT scans (Fig. 5). The opening is partially covered by the preotic pendant (Fig. 1a). The internal carotid artery enters the braincase through the lateral tympanic recess, reaching the pituitary fossa separately from its counterpart.

The subsellar recess is well developed anteroventrally to the basipterygoid process (Fig. 1C). It is continuous with a longitudinal groove excavated ventral to the cultriform process. A similar groove is present in *Coelophysis kayentakatae* (Tykoski, 1998, fig. 12), and *Sinraptor*, although it is separated from the subsellar recess by a transverse bony bar (Paulina Carabajal and Currie, 2012).

The basisphenoidal recess is a well-developed cavity delimited by the basal tubera and the basipterygoid processes. It forms a deep excavation on the ventral

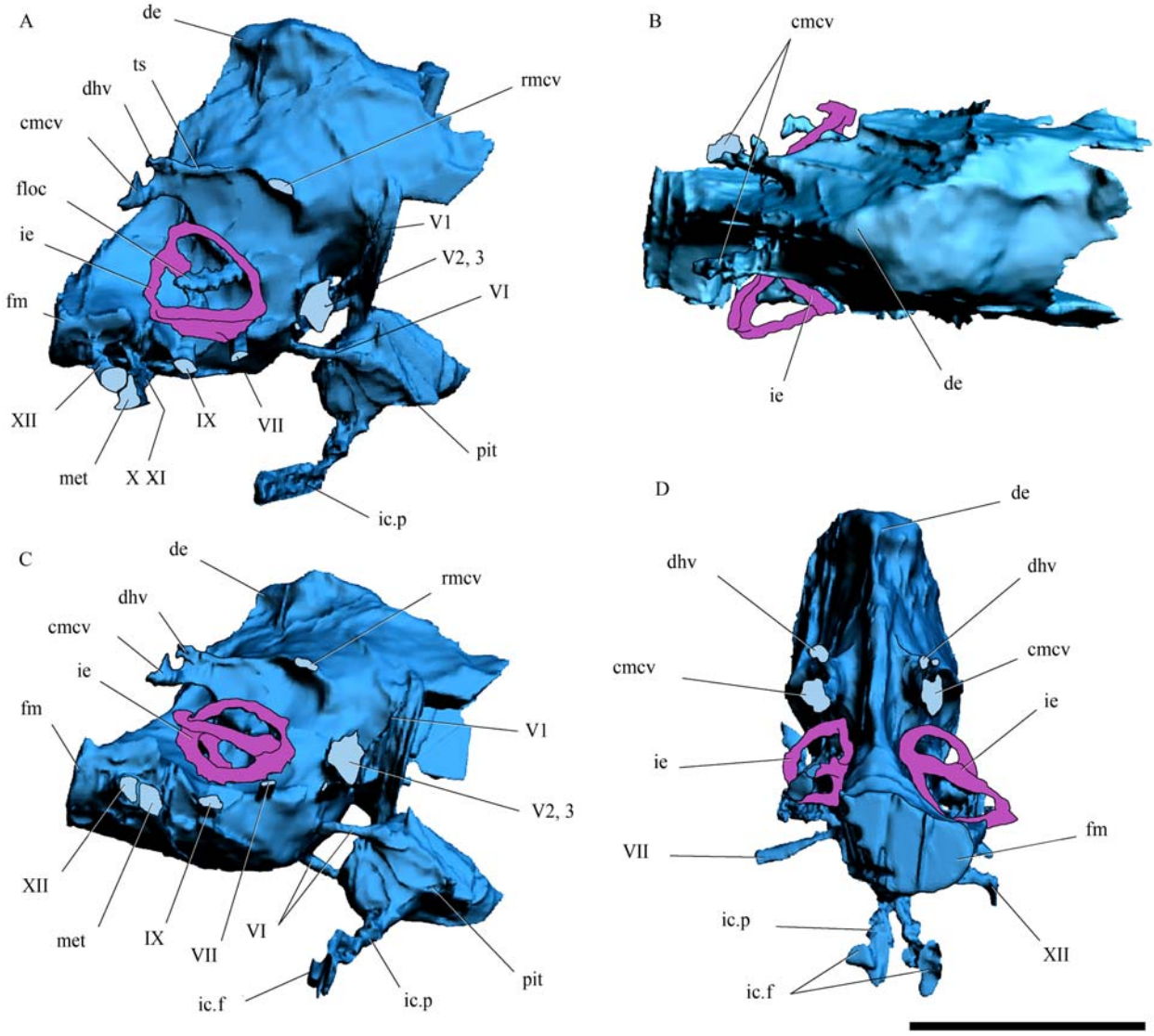

Fig. 6. Surface-rendered CT-based reconstructions of the cranial endocast and endosseous labyrinth of *Sinosaurus triassicus* (ZLJT01) in right lateral (A), posterodorsal (B), lateroventral (C) and posterior (D) views. Abbreviations: cmcv, caudal middle cerebral vein; de, dorsal expansion (dural peak); floc, floccular process; fm, foramen magnum; ic.f, internal carotid artery foramen; ic.p, internal carotid artery passage; ie, inner ear; met, metotic foramen; pit, pituitary cast; rmcv, rostral middle cerebral vein; V, VI, VII, IX, XII, cranial nerves; V1, ophthalmic branch of trigeminal nerve. Scale bar equals 5 cm.

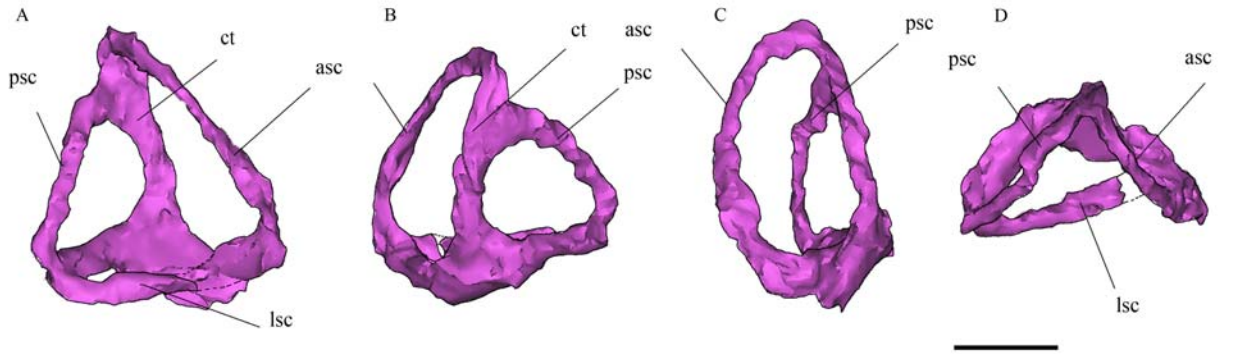

Fig. 7. Digital reconstruction of the right labyrinth of the inner ear of *Sinosaurus triassicus* (ZLJT01) in lateral (A), medial (B), anterior (C) and dorsal (D) views. Abbreviations: asc, anterior semicircular canal; ct, common trunk; lsc, lateral semicircular canal; psc, posterior semicircular canal. Scale bar equals 1 cm.

surface of the basisphenoid (Figs. 1B, 5). The recess is subdivided by a lamina of bone into a main opening posteriorly and a smaller opening just posterior to the basipterygoid processes. The smaller recess (identified as recess "1" in Fig. 5) is transversely developed and delimited by the basipterygoid web anteriorly and a second transverse lamina of bone, which represents an unusual character within theropods.

The basipterygoid recess is less developed (Fig. 1A); it is an oval pit on the lateral side of the basipterygoid process. The CT scans show that the basipterygoid process is solid and that there are no internal cavities.

4 Cranial Endocast

The braincase, brain and inner ear were digitally reconstructed (Figs. 6-7). Because the frontals are not attached to the braincase, the cerebral hemispheres, olfactory tract and olfactory bulbs are not included in the virtual reconstruction. Those structures are preserved as shallow impressions on the ventral aspect of the frontal (Fig. 3A). The olfactory tract is 12 mm long. The impression of the olfactory bulb is oval and divergent in an angle of approximately 45° from the midline.

The preserved cranial endocast of *Sinosaurus* (ZLJT01) is anteroposteriorly 78 mm long, excluding the cerebral hemispheres and olfactory tract and bulbs (57 mm long), which are preserved as impressions in the frontal (Fig. 3A). The endocast would have had a maximum width of 46 mm across the posterior section of the cerebral hemispheres. There are no preserved vascular impressions on the surface of the forebrain, indicating that the dura was thick and the brain was not filling the endocranial cavity (Evans, 2006). As in other basal theropods, such as *Acrocanthosaurus* (Franzosa and Rowe, 2005), *Allosaurus* (Hopson, 1979), *Carcharodontosaurus* (Larsson, 2001), *Ceratosaurus* (Sanders and Smith, 2005), *Giganotosaurus* (Paulina Carabajal, 2010), *Majungasaurus* (Sampson and Witmer, 2007) and *Sinraptor* (Paulina Carabajal and Currie, 2012), the brain parts are arranged serially in a parasagittal row, which is a plesiomorphic condition within theropods (Sampson and Witmer, 2007). In *Sinosaurus*, the hindbrain and midbrain form an angle of approximately 90° (Fig. 6A), as in the carcharodontosaurid *Acrocanthosaurus* (Franzosa and Rowe, 2005). The same angle is obtuse in *Carcharodontosaurus* (Larsson, 2001; Brusatte and Sereno, 2007), *Ceratosaurus* (Sanders and Smith, 2005), *Giganotosaurus* (Paulina Carabajal and Canale, 2010) and *Sinraptor* (Paulina Carabajal and Currie, 2012).

The dorsal section of the endocast corresponds to the dural expansion (dural peak), which is aligned vertically with CN V (Fig. 6A). In *Sinosaurus*, this dural venous sinus is well developed covering the posterior portions of the brain (Sedlmayr, 2002), which is characteristic of many basal theropods (Sampson and Witmer, 2007).

In the lateral view of the endocast, the caudal middle cerebral vein is not closely related to the dural expansion, but is dorsal to CN VII, and close to the midline. The vein is internally convergent with the dorsal head vein, forming a large passage that enters the dorsal expansion (Fig. 6A, C). From the base of the anastomosis of the dorsal head vein, a conspicuous ridge extends anteroventrally along the lateral surface of the endocast, representing the cast of a large transverse vascular sinus (Fig. 6A). A short passage for the rostral middle cerebral vein projects laterally from the dorsal section of this ridge (Fig. 6A,C). The vein exits the braincase through a foramen located close to the prootic-parietal suture, dorsal to CN V. A separated foramen for this vascular element is a derived condition within theropods (Rauhut, 2003; Sampson and Witmer, 2007). In most other theropods, the vein exits the braincase through the same foramen as the trigeminal nerve.

The floccular process (=cerebellar auricle) is a long, narrow structure (Fig. 6A). It projects posteriorly into the ring formed by the anterior semicircular canal, and passes above the level of the common crus of the osseous labyrinth. The cross-section of the base of the floccular process is mediolaterally compressed and is divided into two sections by a constriction, corresponding to the hourglass-shaped floccular recesses of *Aucasaurus* (Paulina Carabajal, 2011a; Paulina Carabajal and Succar, in press) and *Sinraptor* (Paulina Carabajal and Currie, 2012). The base of the medulla oblongata is smooth and, anteriorly, curves dorsally at the level of the dorsum sellae.

The foramina for the second and third cranial nerves are not preserved. The margins of CN IV are partially preserved in the braincase but are not visible in the cranial endocast. All the branches of CN V leave the braincase through a single foramen. Dorsal to CN V there is a passage for the anterior middle cerebral vein. The passages for CN VI, which are clearly visible in the CT scans, are relatively robust compared with the other cranial nerves. They penetrate the pituitary fossa (Fig. 6A,C) as in other theropods, although this condition is unknown in dilophosaurids with preserved braincase. Cranial nerve VII is posterior to and smaller than CN V (Fig. 6A,C). The reconstructed passage for this nerve is straight and projects transversely from the endocast. Cranial nerve IX has a separate opening from those of CN X, CN XI and the jugular vein. Its passage extends from the endocranial cavity to exit the braincase through a

foramen posterior to the columellar recess. In the endocast, CN X–XI form a single root that is semicircular at the base. This represents a cast of the fovea ganglii vasoglossopharyngealis as described for extant birds (Baumel and Witmer, 1993). The branches of CN XII also leave the endocranial cavity through a single foramen. In the endocast, the passage of this nerve is short and robust, and projects laterally (Fig. 6A,C,D).

5 Inner Ear

The endosseous labyrinth of the right inner ear was digitally reconstructed, although it was not possible to reconstruct the morphology of the lagena using the CT scans (Figs. 6-7). The labyrinth is approximately 24.6 mm anteroposteriorly and 26.3 mm dorsoventrally. The three semicircular canals are slender, with tube diameters of approximately 2.2 to 3.0 mm. The common trunk is robust and curves posteriorly whereas the lateral semicircular canal is horizontal. The anterior semicircular canal is oval and 20% larger than the posterior semicircular canal. It extends dorsally above the level of the posterior semicircular canal. This degree of elongation of the anterior semicircular canal reflects its role in stabilizing the head and eyes during bipedal locomotion and is typical of non-avian theropods (Sipla et al., 2004 (I've made this a reference apart), Sanders and Smith, 2005). The posterior semicircular canal is also oval but the main axis is not vertical (Fig. 7B). The angle formed by the anterior and posterior semicircular canals is less than 90° in dorsal view (Fig. 7D), which is similar to the angle observed in *Ceratosaurus* (almost 90°: Sanders and Smith, 2005). The lateral semicircular canal is the smallest; it is oval with the main axis oriented anteroposteriorly.

6 Final Considerations

6.1 Braincase morphology.

The braincase morphology of *Sinosaurus* shares several traits with ceratosaurs (e.g., *Ceratosaurus*), carcharodontosaurids and sinraptorids, principally in the occiput and the basicranium. Some of those characters are the presence of a median tongue-shaped process that posteriorly overlaps a well-developed supraoccipital knob, a posteroventrally oriented and well-developed basisphenoidal recess, and a well-developed subsellar recess and longitudinal groove ventral to the cultriform process. The presence of ossified ethmoidal elements and an interorbital septum, characteristic of ceratosaurs, carcharodontosaurids and sinraptorids, cannot be confirmed in *Sinosaurus*.

The basicranium of *Sinosaurus* is highly pneumatized with four pneumatic recesses: the lateral tympanic recess (poorly developed); the (well-developed) basisphenoidal recess; the basipterygoid recess (shallow but well defined); and the (well-developed) subsellar recess. The ventral surface of the basisphenoid faces strongly posteroventrally as in carcharodontosaurids, sinraptorids and spinosaurids, so that the basisphenoidal recess can be seen in posterior view. The basisphenoidal recess is subdivided into a large cavity posteriorly and a smaller cavity anteriorly. The transverse web of bone that posteriorly delimits this opening is a thinner lamina than the basipterygoidal web. This type of basisphenoidal recess is not present in any other known theropod, and probably represents an autapomorphy for this taxon. The basisphenoidal recess of *Sinraptor dongi* is subdivided, but in this case it separated transversely into a pair of cavities (Paulina Carabajal and Currie, 2012).

Assuming that the skull roof forms a right-angel with the occiput, the resulting occipitofrontal angle (see Coria and Currie, 2002a) for *Sinosaurus* is almost 90°. Sanders and Smith (2005) stated that the obtuse occipitofrontal angle of the braincase and relatively unflexed shape of the endocranium in *Ceratosaurus magnicornis* seem to support a horizontal craniocervical posture. However, the pontine flexure (angel between the midbrain and hindbrain) in *Sinosaurus* is more or less 90° more similar to those of *Coelophysis* (Raath, 1977), *Acrocanthosaurus* (Franzosa and Rowe, 2005, also see Paulina Carabajal and Currie, 2012, figures 7I, J and references herein) and *Allosaurus* (Rogers, 1999), suggesting that it may represent a more conservative endocranial morphology.

6.2 Endocranial morphology

The morphology of the endocranial cast of *Sinosaurus* is anteroposteriorly short and is characterized by marked angles (approximately 90°) between hindbrain, midbrain and forebrain, resembling those observed in other basal theropods such as *Coelophysis rhodesiensis* (Raath, 1977), *Allosaurus* (Rogers, 1999) or *Acrocanthosaurus* (Franzosa and Rowe, 2005). The dorsal expansion, occupied by the venous dorsal longitudinal sinus, is well developed and dorsally projected over the cerebral hemisphere level. The olfactory tract and bulb length is similar to the cerebral hemisphere length, as in *Acrocanthosaurus* and *Sinraptor* (Paulina Carabajal and Canale, 2010, fig. 7D,E), unlike the elongated olfactory tract and bulb (almost twice the length of the cerebral hemisphere) present in *Giganotosaurus carolinii* and ceratosaurs (Paulina Carabajal and Canale, 2010, fig. 7A-C). The flocculus of Sinosaurus is long and blade-shaped, similar to that described in the abelisaurid *Aucasaurus garridoi* (Paulina Carabajal and Succar, in press). The vascular elements

include a common root for the dorsal head vein and the caudal middle cerebral veins, which exit the braincase through separated foramina, whereas the rostral middle cerebral vein exits the braincase separately from the trigeminal nerve.

The morphology of the labyrinth of the inner ear is similar to that described for other basal theropods (e.g. *Allosaurus*, *Ceratosaurus*, *Majungasaurus*). As stated by Sanders and Smith (2005), this conserved configuration is likely a product of similar biomechanical constraints for terrestrial locomotion in these bipedal forms.

7 Conclusions

The braincase of *Sinosaurus triassicus* ZLJT01 shares several traits with that of ceratosaurs, carcharodontosaurids and sinraptorids. The similarities of the braincases of *Sinosaurus* and *Sinraptor* are striking, including the same degree of development of pneumaticity. However, the general brain morphology of *Sinosaurus* is more similar to that of *Coelophysis*, *Acrocanthosaurus* and *Allosaurus*, which have marked angles between the hindbrain, midbrain and forebrain, suggesting that the pattern may represent a more conservative endocranial morphology within basal theropods.

In terms of neuroanatomy, the similarities of the braincase of *Sinosaurus* with that of some allosauroids (basal theropods) are strong, and it would be interesting to do further comparisons of braincase characters within a phylogenetic context to test. Comparisons with other Jurassic basal theropods and phylogenetic analysis of the data are needed to shed light on the distribution of braincase characters within theropods.

Acknowledgements

The authors thank Chairman Laigen Wang (World Dinosaur Valley Park, Yunnan Province, China) for providing the specimen for study. Eva Koppelhus (University of Alberta, Canada) also provided advice and support during the course of this project. CT scanning carried out at the Chaozhou Central Hospital was made possible by Songduan Li.

Manuscript received Dec. 20, 2013
accepted Sept. 22, 2014
edited by Susan Turner and Fei Hongcai

References

Allain, R., 2002. Discovery of a megalosaur (Dinosauria, Theropoda) in the Middle Bathonian of Normandy (France) and its implications for the phylogeny of basal Tetanurae. *Journal of Vertebrate Paleontology*, 22(3): 548–563.

Baumel, J.J., and Witmer, L.M., 1993. Osteologia. In: Baumel, J.J., King, A.S., Breazile, J.E., Evans H.E., and Vanden Berge, J.C. (eds.), *Handbook of avian anatomy: nomina anatomica avium*. Cambridge: Nuttall Ornithological Club, 23: 45–132.

Barsbold, R., and Osmólska, H., 1999. The skull of *Velociraptor* (Theropoda) from the Late Cretaceous of Mongolia. *Acta Palaeontologica Polonica*, 44: 189-219.

Bonaparte, J.F., 1991. The Gondwanian theropod families Abelisauridae and Noasauridae. *Historical Biology*, 5: 1–25.

Brusatte, S.L., and Sereno, P.C., 2007. A new species of *Carcharodontosaurus* (Dinosauria: Theropoda) from the Cenomanian of Niger and a revision of the genus. *Journal of Vertebrate Paleontology*, 27, 902–916.

Chure, D.J., and Madsen, J.H. Jr, 1998. An unusual braincase (? *Stokesosaurus clevelandi*) from the Cleveland-Lloyd Dinosaur Quarry, Utah (Morrison Formation: Late Jurassic). *Journal of Vertebrate Paleontology*, 18(1): 115–125.

Coria, R.A., and Currie, P.J., 2002a. The braincase of *Giganotosaurus carolinii* from the Upper Cretaceous of Argentina. *Journal of Vertebrate Paleontology*, 22 (4): 802–811.

Coria, R.A., and Currie, P.J., 2002b. Un gran terópodo celurosaurio en el Cretácico de Neuquén. *Ameghiniana*, 39(4): 9R.

Currie, P.J., 1985. Cranial anatomy of *Stenonychosaurus inequalis* (Saurischia, Theropoda) and its bearing on the origin of birds. *Canadian Journal of Earth Sciences*, 22: 1643–1658.

Currie, P.J., 1997. Braincase anatomy. In: Currie, P.J., and Padian, K., (eds.) *Encyclopedia of Dinosaurs*. Waltham: Academic Press, 81–83.

Currie, P.J., and Zhao, X.J., 1993. A new carnosaur (Dinosauria, Theropoda) from the Jurassic of Xinjiang, People´s Republic of China. *Canadian Journal of Earth Sciences*, 30: 2037–2081.

Dong, Z.M., 2003. Contributions of new dinosaur materials from China to dinosaurology. *Memoir of the Fukui Prefectural Dinosaur Museum*, 2: 123–131.

Evans, D.C., 2006. Nasal cavity homologies and cranial crest function in lambeosaurine dinosaurs. *Paleobiology*, 32(1): 109–125.

Franzosa, J., 2004. Evolution of the brain in Theropoda (Dinosauria). Unpublished Ph.D. thesis. University of Texas, at Austin, 357 pp.

Franzosa, J., and Rowe, T., 2005. Cranial endocast of the Cretaceous theropod dinosaur *Acrocanthosaurus atokensis*. *Journal of Vertebrate Paleontology*, 25(4): 859–864.

Hopson, J.A., 1979. Paleoneurology. In: Gans, C., (ed.) *Biology of the Reptilia, cap 2 Neurology*. New York: Academic Press, 39–146.

Hu, S.J., 1993. A new Theropoda (*Dilophosaurus sinensis* sp. nov.) from Yunnan, China. *Vertebrata PalAsiatica*, 31: 65–69.

Larsson, H.C.E., 2001. Endocranial anatomy of *Carcharodontosaurus saharicus* (Theropoda, Allosauroidea) and its implications for theropod brain evolution. In: Tanke, D., and Carpenter, K., (eds.). *Mesozoic Vertebrate Life*, Bloomington: Indiana University Press, 19–33.

Lockley, M.G., Li, J.J., Li, R.H., Matsukawa, M., Harris, J.D., and Xing, L.D., 2013. A review of the tetrapod track record in China, with special reference to type ichnospecies:

implications for ichnotaxonomy and paleobiology. *Acta Geologica Sinica* (English edition), 87(1): 1–20.

Madsen, J.H. Jr, 1976. *Allosaurus fragilis*: a revised osteology. *Utah Geological and Mineral Survey Bulletin*, 109, 1–163.

Norell, M.A., Clark, J.M., and Makovicky, P.J., 2001. Phylogenetic relationships among coelurosarian theropods. In: Gauthier, J., and Gall, L.F., (eds). *New Perspectives on the Origin and Early Evolution of Birds*. New Heaven: Yale University Press, 49–67.

Paulina Carabajal, A., 2009. *El neurocráneo de los dinosaurios Theropoda de la Argentina. Osteología y sus implicancias filogenéticas*. Unpublished Ph.D. thesis. La Plata, Facultad de Ciencias Naturales y Museo, Universidad Nacional de La Plata. 540 pp.

Paulina Carabajal, A., 2011a. Braincases of abelisaurid theropods from the Upper Cretaceous of north Patagonia. *Palaeontology*. 54(4): 793–806.

Paulina Carabajal, A., 2011b. The braincase anatomy of *Carnotaurus sastrei* (Theropoda: Abelisauridae) from the Upper Cretaceous of Patagonia. *Journal of Vertebrate Paleontology*, 31: 2, 378–386

Paulina Carabajal, A., and Canale, J.I., 2010. Cranial endocast of the carcharodontosaurid theropod *Giganotosaurus carolinii* Coria and Salgado 1995. *Neues Jahrbuch für Geologie und Paläontologie, Abhandlungen* 258: 249–256.

Paulina Carabajal, A., and Currie P.J., 2012. New information on the braincase and endocast of *Sinraptor dongi* (Theropoda: Allosauroidea): ethmoidal region, endocranial anatomy and pneumaticity. *Vertebrata PalAsiatica*. 50(2): 85–101.

Paulina Carabajal, A., and Succar, C. in press. Brief comments on the endocranial morphology and inner ear of the abelisaurid theropod *Aucasaurus garridoi*. *Acta Palaeontologica Polonica* http://dx.doi.org/10.4202/app.2013.0037

Raath, M.A., 1977. The anatomy of the Triassic theropod *Syntarsus rhodesinensis* (Saurischia: Podokesauridae) and a consideration of its biology. Unpublished Ph.D. thesis, Rhodes University, where in Rhodesia, 123 pp.

Rauhut, O.W.M., 2003. The interrelationships and evolution of basal theropod dinosaurs. *Special papers in palaeontology.* London: The Palaeontological Association, 69: 213.

Rauhut, O.W.M., 2004. Braincase structure of the Middle Jurassic theropod dinosaur *Piatnitzkysaurus*. *Canadian Journal of Earth Sciences*, 41: 1109–1122.

Rogers, S.W., 1999. *Allosaurus*, crocodiles and birds: evolutionary clues from espiral computed tomography of an endocast. *Anatomical Record*, 257: 162–173.

Rowe, T., 1989. A new species of the theropod dinosaur *Syntarsus* from the Early Jurassic Kayenta Formation of Arizona. *Journal of Vertebrate Paleontology*, 9(2): 125–136.

Sampson, S.D. and Witmer, L.M. 2007. Craniofacial anatomy of *Majungasaurus crenatissimus* (Theropoda: Abelisauridae) from the Late Cretaceous of Madagascar. *Journal of Vertebrate Paleontology*, 8(2): 32–102.

Sanders, R.K., and Smith, D.K., 2005. The endocranium of the theropod dinosaur Ceratosaurus studied with computed tomography. *Acta Paleontologica Polonica*, 50 (3): 601–616.

Sedlmayr, J.C., 2002. *Anatomy, evolution, and functional significance of cephalic vasculature in Archosauria.* Unpublished Ph.D. thesis, Ohio University, Athens, Ohio, 398 pp.

Sipla, J., Georgi, J., and Forster, C., 2004. The semicircular canals of dinosaurs: tracking major transitions in locomotion. *Journal of Vertebrate Paleontology*, 24(Supplement):113A (abstract).

Smith, N.D., Makovicky, P.J., Hammer, W.R., and Currie P.J., 2007. Osteology of *Cryolophosaurusellioti* (Dinosauria: Theropoda) from the Early Jurassic of Antarctica and implications for early theropod evolution. *Zoological Journal of the Linnean Society*, 151: 377–421

Sues, H.D., Frey, E., Martill, D.M., and Scott, D.M., 2002. *Irritator challengeri*, a spinosaurid (Dinosauria: Theropoda) from the Lower Cretaceous of Brazil. *Journal of Vertebrate Paleontology*, 22, 535–547.

Taquet, P., and Welles, S.P., 1977. Redescription du crâne de dinosaure théropode de Dives (Normandie). *Annales de Paléontologie (Vertébrés)*, 63, 191–206.

Tykoski, R.S., 1998. The osteology of *Syntarsus kayentakatae* Syntarsus kayentakatae and its and its implications for ceratosaurid phylogeny. Unpublished M.S. Thesis, University of Texas at Austin, 434 pp.

Welles, S.P., 1984. *Dilophosaurus wetherilli* (Dinosauria, Theropoda) osteology and comparisons. *Palaeontographica Abteilung A*, 185, 85–180.

Witmer, L.M., Ridgely, R.C., Dufeau, D.L., Semones, M.C., 2008. Using CT to peer into the past: 3D visualization of the brain and ear regions of birds, crocodiles, and nonavian dinosaurs. In: Endo, H., and Frey, R. (eds.), Anatomical Imaging: Towards a New Morphology. Springer-Verlag, Tokyo. Pp. 67–88

Witmer, L.M., and Ridgely, R.C., 2010. The Cleveland tyrannosaurid skull (*Nanotyrannus* or *Tyrnnosaurus*): new findings based on CT Scanning, with special reference to the braincase. *Kirtlandia*, 57: 61–81.

Xing, L.D., Harris, J.D., Toru, S., Masato, F., and Dong, Z.M., 2009. Discovery of dinosaur footprints from the Lower Jurassic Lufeng Formation of Yunnan Province, China and New Observations on Changpeipus. *Geological Bulletin of China*. 28(1): 16–29.

Xing, L.D., 2012. *Sinosaurus* from southwestern China. Unpublished Master of Science Thesis. Edmonton: University of Alberta, 286 pp.

Xing, L.D., Bell, P.R., Rothschild, B.M., Ran, H., Zhang, J.P., Dong, Z.M., Zhang, W., and Currie, P.J., 2013. Tooth loss and alveolar remodeling in *Sinosaurus triassicus* (Dinosauria: Theropoda) from the Lower Jurassic strata of the Lufeng Basin, China. *Chinese Science Bulletin* (English Version), 58 (16): 1931–1935.

Xing, L.D., Wang, Y.K., Snively, E., Zhang, J.P., Dong, Z.M., Burns, M.E., and Currie, P.J. In press. Model-Based Identification of Mechanical Characteristics of *Sinosaurus* (Theropoda) Crests. *Acta Geologica Sinica* (English edition).

About the first author

Xing Lida, A Ph. D. student from School of the Earth Sciences and Resources, China University of Geosciences, Beijing; Focus on theropods osteology and dinosaur tracks in China.